# A Continuation Method for computation of H $\infty$ gains of Linear Continuous-Time Periodic Systems

Paul Rousse, John Hauser, Pierre-Loïc Garoche

# A Continuation Method for computation of $H_\infty$ gains of Linear Continuous-Time Periodic Systems

Paul Rousse*, John Hauser** and Pierre-Loïc Garoche*

***Abstract*— A continuation method is applied to compute the $H_\infty$ gain of a periodic linear system. The $H_\infty$ gain of a periodic linear system can be equivalently found by solving a Periodic Differential Riccati Equation (PDRE) for an increasing sequence of gain candidates until no solution exists. Solving the PDRE can be cumbersome. However, for a null gain candidate, the PDRE is a Periodic Differential Lyapunov Equation (PDLE) that can be solved efficiently. Similarly, for a small increase in the gain candidate, the solution can be approximated by solving another PDLE. We describe an application of the continuation method where the corrector uses a Boundary Value Problem solver. Therefore, using a continuation method can be promising for such a problem. The gain candidate is increased until no solution to the PDRE exists. Compared to Hamiltonian based approaches, our approach suffers less from ill-conditioned differential equations for systems where the periodicity is long compared to the dynamic of the system of interest.**

## I. Introduction

Periodic systems appear frequently in physical systems as in [1], [2], and [3]. Their analysis remains challenging. They exhibit behaviors of Linear Parameter Varying systems as well as discrete-time systems.

Computation of $H_\infty$ norm for linear periodic systems has been studied using the Hamiltonian system e.g. [5]. The transition matrix of the Hamiltonian system is computed over one time period for a given $H_\infty$ gain candidate. Such an approach has disadvantages. The Hamiltonian matrix is ill-conditioned (it has stable and unstable parts) and therefore accurate computation of the transition matrix is difficult to achieve, in the general case. Many efforts have been devoted to improve numerical accuracy. This approach [5] relies on the group property of the transition matrix: the time interval over one period is partitioned and the transition matrix is computed over each interval. The transition matrix is then obtained as the product of each transition matrix computed along the time partition.

In another approach [6], the time-dependent system matrices are projected over a non-finite frequency domain basis. The lifted system is a Linear Time-Invariant system, then, a finite-dimensional approximation of the system is obtained by projecting over the low-frequencies. Finally, the $H_\infty$ gain of this LTI system is a good approximation of the $H_\infty$ gain of the original periodic linear system.

A third approach amounts to solve a Periodic Differential Riccati Equation (associated with the Hamiltonian system previously cited). Since solutions of the Differential Riccati Equation (DRE) might have finite escape time, finding a periodic solution can be difficult. However, solutions vary according to a Periodic Differential Lyapunov Equation for small variations of the PDRE's parameters. Continuation methods have been successfully used to compute complex solutions for subclasses of the family of Riccati equations as in [7] (for a perturbed Lyapunov equation), [8] (for a DRE), [9] (for Algebraic Riccati Equation), and [10] (for modified Algebraic Riccati Equation). In practice, finding the solution to the PDRE is complex as it involves a numerical integration of the DRE plus a boundary constraint over this solution. In this paper, we use the continuation method to solve the PDRE for the specific case of $H_\infty$ gain computation. We follow the curve of solutions to the PDRE when the gain candidate varies from $\infty$ to the actual $H_\infty$ gain of the system. The implicit function theorem guarantees the existence of the solution along the curve (see Theorem 4.E in Chapter 4.8 of [11]).

*Contributions:* We propose an application of the continuation method to solve the PDRE in the specific case of $H_\infty$ norm computation. Up to the knowledge of the author, such an approach has not been investigated in the past.

*Plan:* Section II defines the $H_\infty$ norm computation problem for periodic linear systems. Section III proposes a continuation method approach to address this problem. Section IV details our implementation of the continuation method. Section V treats the norm computation for a toy example and a flying wing aircraft model.

*Notation:* $\mathcal{C}^0(I;\ \mathbb{R}^{n\times m})$ (resp. $\mathcal{C}^1(I;\ \mathbb{R}^{n\times m})$) is the set of continuous functions over $I$ (resp. continuous, differentiable, and of continuous derivative over $I$) from $I$ to $\mathbb{R}^{n\times m}$. $\mathcal{L}_2(\mathbb{R}^+;\mathbb{R}^n)$ is the set of square-integrable functions from $\mathbb{R}^+$ to $\mathbb{R}^n$. $\mathbb{S}^{n\times n}$ is the set of square symmetric matrices of size $n$. For a function $f$ of $n$ arguments, $D_i f$ is its differential with respect to the $i^{th}$ argument. For a given time-dependent square matrix $A(\cdot) \in \mathcal{C}^0(\mathbb{R}^+;\ \mathbb{R}^{n\times n})$, its transition matrix $\Phi_A(\cdot,\cdot)$ is the time-dependent matrix, defined over $\mathbb{R}^+\times\mathbb{R}^+$, solution of $\dot{\Phi}_A(t,\tau) = A(t)\Phi_A(t,\tau)$, for $t,\tau \in \mathbb{R}^+$, with initial condition $\Phi_A(\tau,\tau) = I_n$ where $I_n \in \mathbb{R}^{n\times n}$ is the identity matrix. For a $T$-periodic $A(\cdot)$, $T > 0$, $\Phi_A(T,0)$ is the *monodromy matrix* of $A(\cdot)$.

## II. $H_\infty$ Norm Computation

Let $G$ be the $T$-periodic linear system that associates to a noise $\mathbf{w} \in \mathcal{L}_2(\mathbb{R}^+;\mathbb{R}^m)$, the output $\mathbf{y} = G \circ \mathbf{w} \in$

*ONERA, Toulouse, 31000, France (e-mail: {Paul.Rousse,Pierre-Loic.Garoche}@onera.fr); **University of Colorado Boulder, Boulder, CO 80309, USA (e-mail: John.Hauser@colorado.edu).

$\mathcal{L}_2(\mathbb{R}^+;\mathbb{R}^p)$ defined by

$$G : \begin{cases} \dot{\mathbf{x}} = A(t)\mathbf{x} + B(t)\mathbf{w} \\ \mathbf{y} = C(t)\mathbf{x} \end{cases} \tag{1}$$

where $A(\cdot)$, $B(\cdot)$ and $C(\cdot)$ are $T$-periodic Lipschitz matrix functions (i.e. $X(t+T) = X(t)$ for any $t \in \mathbb{R}$ where $X \in \{A, B, C\}$), of size $n \times n$, $n \times p$ and $m \times n$ (resp.) defined over $\mathbb{R}$, such that $A(\cdot)$ is exponentially stable, $(A(\cdot), B(\cdot))$ is controllable and $(A(\cdot), C(\cdot))$ detectable. The $H_\infty$ norm defined by

$$\|G\|_\infty = \quad \text{Supremum} \quad \frac{\|G \circ \mathbf{w}\|_2}{\|\mathbf{w}\|_2} \tag{2}$$

The $H_\infty$ gain of $G$ cannot be directly computed using (2). Classically, the equivalent following dual constrained optimization problem is solved instead of (2)

$$\begin{aligned} &\text{Infimum } \gamma \\ &\text{Such that } \frac{\|G \circ \mathbf{w}\|_2}{\|\mathbf{w}\|_2} \leq \gamma \end{aligned} \tag{3}$$

For a given $\gamma \geq 0$, the constraint in (3) is equivalent to showing that

$$\begin{aligned} &\text{Infimum} \quad \int_0^\infty \gamma^2 \|\mathbf{w}(t)\|^2 - \|\mathbf{y}(t)\|^2 dt \\ &\text{Such that} \quad \mathbf{y} = G \circ \mathbf{w} \end{aligned} \tag{4}$$

has a positive solution.

Checking that $\|G\|_\infty < \gamma$ for a given gain-candidate $\gamma > 0$ is equivalent to the existence of a symmetric, $T$-periodic, and positive definite solution $P$ to the following Periodic Differential Riccati Equation (PDRE)

$$\begin{cases} 0 = \dot{P} + A(t)^\top P + PA(t) \\ \qquad + C(t)^\top C(t) + \alpha P B(t) B(t)^\top P \\ P(0) = P(T) \end{cases} \tag{5}$$

where $\alpha = \frac{1}{\gamma^2}$. Such a result is stated in Chapter 6, Theorem 6.14 of [12] in the case of linear continuous time-periodic systems[1]. In this work, we propose a continuation method to solve the following optimization problem (equivalent to (3))

$$\begin{aligned} \alpha^* = \quad &\text{Supremum} \quad \alpha \\ &\text{Such that} \quad \textit{there is a positive definite } T\textit{-periodic solution } P(\cdot) \textit{ to } (5) \end{aligned} \tag{6}$$

Then, the $H_\infty$ norm of $G$ is equal to $\frac{1}{\sqrt{\alpha^*}}$.

*Remark 1:* In Hamiltonian based approaches, the LQR problem (4) is solved by finding the optimal $\mathbf{w}^*$ of (4). Such $\mathbf{w}^*$ is obtained by computing the monodromy matrix $\Phi_H(T, 0)$ (see the Notation paragraph at the end of Section I)) of the Hamiltonian matrix $H(t) = \begin{bmatrix} A(t) & \alpha B(t)B(t)^\top \\ -C(t)^\top C(t) & -A(t)^\top \end{bmatrix}$. $H(\cdot)$ is known to be symplectic (see 6.3.1.2 in [12]) and therefore any stable eigenvalue of $H(\cdot)$ is associated to an unstable eigenvalue. This property leads to numerical instabilities when the period $T$ of $G$ is large compared to the characteristic time constant of $G$'s dynamic. By using (5) to solve (4), we avoid such numerical problems of Hamiltonian based methods. More details are given in Section V-A.

[1] In [12], the PDRE is formulated with $\tilde{P} = \gamma^2 P^{-1}$.

## III. Continuation method for $H_\infty$ gain computation

Let $\mathcal{R} : \mathcal{C}^1(\mathbb{R}; \mathbb{S}^{n\times n}) \times \mathbb{R}^+ \to \mathcal{C}^0(\mathbb{R}; \mathbb{S}^{n\times n})$ be such that

$$\begin{aligned} \mathcal{R}(P(\cdot), \alpha) = &\dot{P}(\cdot) + A(\cdot)^\top P(\cdot) + P(\cdot)A(\cdot) \\ &+ C(\cdot)^T C(\cdot) + \alpha P(\cdot) B(\cdot) B(\cdot)^T P(\cdot). \end{aligned}$$

We study the curve $\alpha \to P_\alpha(\cdot)$ of $T$-periodic symmetric matrix $\mathcal{C}^1$ functions[2] that satisfies

$$\mathcal{R}(P_\alpha(\cdot), \alpha) = 0. \tag{7}$$

The next paragraphs motivate the use of continuation methods to find the $H_\infty$ norm of $G$. They introduce preliminary theoretical background necessary for the implementation of the method. We give existence conditions of the curve $\alpha \to P_\alpha(\cdot)$ over an interval $[0, \alpha^*)$, $\alpha^* > 0$. For any $\alpha \in (0, \alpha^*)$, the $H_\infty$ gain of $G$ is overapproximated by $1/\sqrt{\alpha}$, i.e. $\|G\|_\infty \leq \frac{1}{\sqrt{\alpha}}$; and when $\alpha = \alpha^*$, no positive definite solution exists and therefore $\|G\|_\infty = \frac{1}{\sqrt{\alpha^*}}$. Section IV is devoted to an implementation that evaluates such $\alpha^*$.

*Existence of $P_0(\cdot)$:* The equation $\mathcal{R}(P_0(\cdot), 0) = 0$ is a PDLE where $A(\cdot)$ is stable and $(C(\cdot), A(\cdot))$ is observable. By the Lyapunov Theorem (see the Extended Lyapunov lemma in Chapter 6, Section 2.3.1 of [12]), a $T$-periodic solution $P_0(\cdot)$ exists, is unique, and is positive definite over $\mathbb{R}$.

*Existence of $P_\alpha(\cdot)$ over $\alpha \in [0, \alpha^*)$:* To prove the existence of $P_\alpha(\cdot)$ for greater values than $\alpha = 0$, we apply the implicit function theorem to (7) (as described in Chapter 4.8 of [11]). The implicit function theorem guarantees that if the curve $\alpha \to P_\alpha(\cdot)$ exists at some given $\alpha$, it locally exists on a neighborhood $I$ of $\alpha$ when $\mathcal{R}$ is differentiable at $(P_\alpha(\cdot), \alpha)$ and its differential $Q \mapsto D_1\mathcal{R}(P_\alpha(\cdot), \alpha) \cdot Q$ is invertible. We now detail the computation of $D_1\mathcal{R}$ and explicit conditions of $Q \mapsto D_1\mathcal{R}(P_\alpha(\cdot), \alpha) \cdot Q$ to be invertible.

Let us assume that a $T$-periodic $P_\alpha(\cdot)$ exists for a given $\alpha \geq 0$. By differentiating $\mathcal{R}$ with respect to $\alpha$, it holds

$$D_1\mathcal{R}(P_\alpha(\cdot), \alpha) \cdot Q_\alpha(\cdot) + D_2\mathcal{R}(P_\alpha(\cdot), \alpha) = 0 \tag{8}$$

where $Q_\alpha(\cdot)$ is a $T$-periodic symmetric matrix function. $Q_\alpha(\cdot)$ corresponds to the tangent vector of the curve $\alpha \to P_\alpha(\cdot)$ at $\alpha$. When the tangent $Q_\alpha(\cdot)$ is well defined in the vector space of symmetric $T$-periodic matrix functions, the curve $\alpha \to P_\alpha(\cdot)$ is defined in the neighborhood of $\alpha$

[2] The operator $\mathcal{R}$ is defined in the vector space of differentiable $P(\cdot)$ functions. However, $\mathcal{R}$ could have been defined in its integral form for continuous (not necessarily differentiable) functions $P(\cdot)$. E.g. $\mathcal{R}_i(P(\cdot), \alpha) = r(\cdot)$ where $r(t) = P(t) - P(0) + \int_0^t \left(A(s)^\top P(s) + P(s)A(s) + C(s)^T C(s) + \alpha P(s)B(s)B(s)^T P(s)\right) ds$. We chose the differential form for readability.

(application of the implicit function theorem in Chapter 4.8 of [11]).

Using variational calculus over (7) (see Chapter 2.1 of [11]), we can explicitly derive (8). The tangent vector $Q_\alpha(\cdot)$ satisfies the following Periodic Differential Lyapunov Equation (PDLE)

$$\begin{cases} 0 = \dot{Q}_\alpha + Q_\alpha F_\alpha(t) + F_\alpha(t)^\top Q_\alpha + P_\alpha(t)B(t)B(t)^\top P_\alpha(t) \\ Q_\alpha(T) = Q_\alpha(0) \end{cases} \tag{9}$$

where

$$F_\alpha(\cdot) = A(\cdot) + \alpha B(\cdot)B(\cdot)^\top P_\alpha(\cdot) \tag{10}$$

and $Q_\alpha(\cdot)$ a $T$-periodic function of $\mathcal{C}^1(\mathbb{R};\mathbb{S}^{n\times n})$. Solutions of (9) are known (see Chapter 6 of [12]) to satisfy

$$\begin{aligned} Q_\alpha(t) =& \Phi_\alpha(t,0)^\top Q_\alpha(0)\Phi_\alpha(t,0) \\ &+ \int_0^t \Phi_\alpha(t,s)^\top U_\alpha(s)\Phi_\alpha(t,s)ds \end{aligned} \tag{11}$$

where $\Phi_\alpha(\cdot,\cdot)$ is the transition matrix of $F_\alpha(\cdot)$ and $U_\alpha(\cdot) = P_\alpha(\cdot)B(\cdot)B(\cdot)^\top P_\alpha(\cdot)$. The invertibility of $D_1\mathcal{R}$ at $(P_\alpha(\cdot),\alpha)$ is equivalent to the existence of a periodic solution $Q_\alpha(\cdot)$ to (11) for any $U_\alpha(\cdot)$, i.e. if

$$X \to X - \Phi_\alpha(T,0)^\top X \Phi_\alpha(T,0)$$

is invertible, then $D_1\mathcal{R}$ is invertible and $\alpha \to P_\alpha(\cdot)$ exists in the neighborhood of $\alpha$.

Let us study the map $\mathcal{L}$ over $\mathbb{S}^{n\times n}$

$$\mathcal{L} : X \to X - \Phi_\alpha(T,0)^\top X \Phi_\alpha(T,0). \tag{12}$$

For a $Y = \mathbb{S}^{n\times n}$, the equation $\mathcal{L}(X) = Y$ is a Discrete-Time Lyapunov Equation. $\mathcal{L}$ has $n^2$ eigenvalues which are $1-\lambda_i\lambda_j^*$ where $\lambda_i, \lambda_j$ are eigenvalues of the monodromy matrix $\Phi_\alpha(T,0)$ of $F_\alpha(\cdot)$. Therefore, as long as $\Phi_\alpha(T,0)$ has no eigenvalues on the unit disk, the linear operator $\mathcal{L}$ is invertible. This condition can be equivalently stated by: if $F_\alpha(\cdot)$ is stable, the tangent $Q_\alpha(\cdot)$ is defined.

Let $\alpha$ s.t. $F_\alpha(\cdot)$ is exponentially stable, then the tangent $Q_\alpha(\cdot)$ exists and is positive definite. Therefore, the curve $\alpha \to P_\alpha(\cdot)$ is monotonically increasing (i.e. for any $\alpha' > \alpha$, $P_{\alpha'}(\cdot) \succeq P_\alpha(\cdot)$ over $\mathbb{R}$). There is a $\tilde{\alpha} > 0$ such that $F_{\tilde{\alpha}}(\cdot)$ is not stable. Let $\alpha^*$ be the maximal value such that $F_\alpha(\cdot)$ is stable over $\alpha \in [0,\alpha^*)$. The curve $\alpha \to P_\alpha(\cdot)$ is therefore continuously defined over the interval $[0,\alpha^*)$. It follows

*Theorem 1:* There is a $\alpha^* > 0$ s.t. $P_\alpha(\cdot)$ is a symmetric positive definite $T$-periodic function for any $\alpha \in [0,\alpha^*)$ satisfying

$$0 = \dot{P}_\alpha + A(\cdot)^\top P_\alpha + P_\alpha A(\cdot) + C(\cdot)^T C(\cdot) + \alpha P_\alpha B(\cdot)B(\cdot)^T P_\alpha.$$

*Proof:* The existence of the curve over $[0,\alpha^*)$ follows from the implicit function theorem applied to $\mathcal{R}$ in the vector space of symmetric $T$-periodic matrix function and reals. ■

## IV. Implementation

$P_0(\cdot)$ and $Q_\alpha(\cdot)$ (for a given $P_\alpha(\cdot)$) are solutions of a PDLE and can be numerically evaluated since it only requires numerical integration and solving a Discrete-Time Lyapunov Algebraic Equation (as detailed in Section III). Therefore, the curve $\alpha \to P_\alpha(\cdot)$ is well defined at $\alpha = 0$ and its tangent can be evaluated at any $P_\alpha$. This is the ideal playground for continuation methods (as described in [13]). We now describe our implementation of the continuation method for $H_\infty$ norm computation. We follow the curve $P_\alpha(\cdot)$ that satisfies (7) for increasing values of $\alpha$ until the implicit function theorem is not applicable, i.e. until $F_\alpha(\cdot)$, defined in (10), becomes unstable.

Classical implementations of the continuation method involve 3 steps: a prediction step, a correction step, and a step size control step. In the prediction step, the tangent of the curve is used to compute a first-order prediction of the next point on the curve. The correction step projects the first-order prediction on the curve, it is usually implemented with a root-finding algorithm that solves (7) for the current point. Finally, the step size is adapted according to local geometric measurements of the curve and/or to convergence rates within the correction step's algorithm.

The next paragraphs give more details about the prediction, the correction, and the step size control steps. Our implementation is substantially inspired by [13] with an additional mechanism in the step size control.

At each iteration, we compute the solution $P_k$ to the PDRE for the current gain candidate $\alpha_k$. The prediction $\widetilde{P}_k$ is the first-order approximation $\widetilde{P}_k = P_{k-1} + h_k Q_k$ where $\tilde{Q}_k$ is the solution to the PDLE (9) and $h_k = \alpha_k - \alpha_{k-1}$ is the step size.

*Prediction:* is based on a first-order prediction $\widetilde{P}_{k+1}$

$$\widetilde{P}_{k+1} = P_k + h_k Q_k$$

where $Q_k$ is the current tangent vector.

*Corrector:* The corrector step is implemented with a Boundary Value Problem (BVP) solver to find the periodic solution of (5). Our implementation uses the `bvp5c` solver (see [14]). The BVP solver implements a Newton method coupled with a numerical integration scheme to solve the root-finding problem $P_T(P_0) - P_0 = 0$ where $P_T$ associates to an initial value $P_0$ the value at $T$ of the solution $P(\cdot)$ to the ODE in (5). When the BVP's Newton method does not converge, the step size is divided by a factor 2.

*Step Control:* In light of Chapter 6 in [13], our step control algorithm is based over local measurements of the geometry of $\{(P(\cdot),\alpha) \mid \mathcal{R}(P(\cdot),\alpha) = 0\} \subset \mathcal{C}^1(\mathbb{R};\mathbb{S}^{n\times n}) \times \mathbb{R}$. These measurements are compared to user-defined parameters and the step size is controlled accordingly.

$\kappa_k = \frac{\|Q_k(0)\|}{\|Q_{k-1}(0)\|}$ measures the contraction of $P_k(0)$ between two iterations. $\beta_k = angle(Q_k(0), Q_{k-1}(0))$ measures the angle of the tangent vector between two iterations[3], $\beta_k$ is related to the measurement of the local curvature (see [13]).

The step size is controlled such that the measurements $\kappa_k$ and $\beta_k$ respectively converge to the user-defined parameters

[3]The $angle$ function over matrices is defined using the regular arc cosinus function $arccos$ as follows $angle(A,B) = arccos\left(\frac{\langle A,B\rangle}{\|A\|\|B\|}\right)$ where $\langle A,B\rangle = trace(A^\top B)$ is a scalar product over the set of matrices and $\|\cdot\|$ is its induced norm s.t. $\|A\| = \sqrt{trace(A^\top A)}$.

$\kappa^0$ and $\beta^0$. Let

$$\tilde{f}_k = \max\left\{\frac{\kappa_k}{\kappa^0}, \frac{\beta_k}{\beta^0}\right\}$$

be the contracting ratio of the step size. To bound the variations of the step size, the actual contracting ratio of the step size is chosen as the saturated $\tilde{f}_k$ within the bounds $\left[\frac{1}{2}, 2\right]$ $f_k = \max\left\{\min\left\{\tilde{f}_k, 2\right\}, \frac{1}{2}\right\}$. At the next iteration, the step size would be $h_{k+1} = \frac{h_k}{f_k}$. Contrary to [13], the corrector's step size contraction is measured with the actual step of the Newton iteration method.

When the correction step fails, we cannot conclude that the corresponding PDRE is unsolvable, i.e. we don't know if $\alpha^* < \alpha_k$. Therefore, $\alpha_k$ is used as an upper bound only for the next step only (and not all the remaining steps). We implement it as follows:

- at each iteration, when the correction step fails to find a solution for a given $\alpha_k$, we use $\bar{\alpha} = \alpha_k$ as an upper bound for the next iteration;
- when the correction step successfully find a solution, this upper bound is reset (i.e. $\bar{\alpha} = \infty$).

**Algorithm 1:** Continuation algorithm for $H_\infty$ gain computation.

**Data:** $(A(\cdot), B(\cdot), C(\cdot))$: a $T$-periodic linear system
$T$: the period
tol: the tolerance

**Result:** $\tilde{\alpha}$ an approximation of $\alpha$

$P_0 =$ `solve_PDLE`$(A, C)$ ; *// Initial solution of the PDRE for $\alpha = 0$*
$h = 1$ ; *// Initial step size*
$\alpha_0 = 0$ ; *// Initial $\alpha$*
$k = 0$ ; *// iteration step*
**while** $|\alpha_k - \alpha_{k-1}| \leq tol$ **do**
  */* Prediction step */*
  $F_k = A + \alpha_k BB^\top P_k$ ;
  $U_k = P_k BB^\top P_k$ ;
  $Q_k =$ `solve_DTLE`$(F_k, U_k)$ ; *// Evaluation of PDRE's differential at $(P_k, \alpha_k)$*
  $\widetilde{P}_{k+1} = P_k + hQ_k$ ; *// Prediction of the solution to the PDRE*
  */* Correction step (BVP Solver) */*
  $(\overline{P}_{k+1}, accept\_step) =$ `solve_PDRE`$(\widetilde{P}_{k+1})$ ; *// Solve the PDRE equation for the initial guess $\widetilde{P}_{k+1}$*
  */* Step Control */*
  compute $\kappa_k$ and $\beta_k$;
  */* Next Iteration */*
  **if** *accept_step* **then**
    $P_{k+1} = \overline{P}_{k+1}$;
    $h_{k+1} = min(\frac{h_k}{f}, \bar{\alpha}_k - \alpha_k)$ ; *// application of the step control*
    $k = k + 1$;
    $\bar{\alpha}_k = \infty$; *// reset $\alpha$'s upper bound*
  **else**
    $\bar{\alpha}_k = \alpha_k$ ; *// temporary upper bound of $\alpha$*
    $h_k = \frac{h_k}{2}$; *// step refused, reduce the step size*
  **end**
**end**

*Algorithm:* Algorithm 1 describes our implementation of the continuation method for the computation of the $H_\infty$ gain of a $T$-periodic system $G = (A(\cdot), B(\cdot), C(\cdot))$.

Fig. 1. Each dot corresponds to an iteration in Algorithm 1. The sequence of $\{\alpha_k\}$ converges to $\alpha^*$ solution of (3). Each red star corresponds to an *accepted* solution of the BVP solver (i.e. the Newton algorithm of the BVP solver converged to a solution $P_k(\cdot)$ to (5) with a residual below $10^{-6}$), each blue dot is *non-accepted* one.

## V. Example

We use the implementation in Algorithm 1 of the continuation method detailed in Section IV to compute the $H_\infty$ norm of two systems. Section V-A treats the case of a simple 2D toy example. Section V-B studies a flying wing aircraft model.

### A. Toy example

We study the $T$-periodic system $G$ as defined in (1) with the following parameters

$$\begin{cases} A(t) = A_0 + A_1 \sin(2\pi t) \\ B(t) = B_0 + B_1 \cos(2\pi t) \\ C(t) = \begin{bmatrix} 1 & 1 \end{bmatrix} \end{cases}$$

with

$$A_0 = \begin{bmatrix} -1 & 0.3 \\ -0.7 & -0.3 \end{bmatrix}, \qquad A_1 = \begin{bmatrix} 1 & 0 \\ 0 & 0.3 \end{bmatrix},$$
$$B_0 = \begin{bmatrix} -1 & 2 \end{bmatrix}^\top \quad \text{and} \quad B_1 = \begin{bmatrix} 0.1 & 0 \end{bmatrix}^\top.$$

$(A(\cdot), B(\cdot), C(\cdot))$ are $T$-periodic matrix function with $T = 1$. Using Algorithm 1 that implements the continuation method described in Section III and IV to solve (3), we find $\alpha^* = 0.028326$ and therefore the $H_\infty$ norm of $G$ is $\|G\|_\infty = 5.9416$.

Figure 1 shows the sequence $\{\alpha_k\}_k$ determined with the continuation algorithm. As $\alpha$ goes from 0 to $\alpha^*$, one of the eigenvalues converges to the unit disk. Figure 2 plots the root locus of $\Phi_\alpha(T, 0)$ ($F_\alpha(\cdot)$'s monodromy matrix) when $\alpha$ goes from 0 to $\alpha^*$. When $\alpha = \alpha^*$, eigenvalues intersect the unit circle of the complex plane. Trajectories associated to these eigenvalues are neutral. Figure 3 plots some internal values used in the continuation method's Algorithm 1. When $\alpha \to \alpha^*$, the curvature $\beta_k$ at the $k^{th}$ iteration diverges and the Jacobian of the BVP solver gets closer to noninvertibility. These behaviors can be explained in light of (12). Since $F_\alpha(\cdot)$ is neutrally stable (and not exponentially stable) when $\alpha = \alpha^*$, eigenvalues its monodromy matrix $\Phi_\alpha(T)$ get closer to the unit circle and therefore the associated linear operator $\mathcal{L}_\alpha$ defined in (12) becomes noninvertible. The tangent vector $Q_\alpha(\cdot)$, which requires $\mathcal{L}_\alpha$ to be invertible, diverges. However, even if the tangent $Q_\alpha$ diverges at $\alpha^*$, the solution $P_\alpha(\cdot)$ does not seems to diverge (see Figure 4).

These observations should be compared to a Hamiltonian approach. For this example, eigenvalues of the Hamiltonian matrix (as defined in Remark 1) for $\alpha = \alpha^* \pm 1 \cdot 10^{-10}$ have a maximal absolute value of 0.9 when $t \in [0, T]$. Since the monodromy matrix is the solution of a linear system with the Hamiltonian as a dynamic matrix, in the worst case, eigenvalues of $\Phi_H(T, 0)$ are equal to $\exp\left(|\overline{\lambda}|T\right)$ where

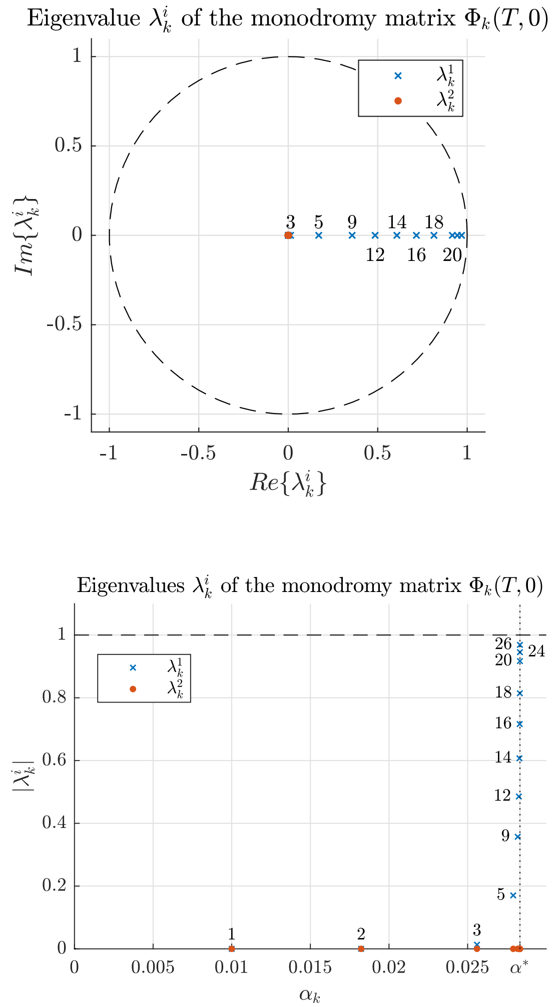


Fig. 2. Eigenvalues of the monodromy matrix $\Phi_k(T,0)$ of $F_k(\cdot)$ defined in (10) for $\alpha = \alpha_k$. The iteration number $k$ is written near the eigenvalue $\lambda_k^1$. As $\alpha_k$ goes to $\alpha^*$, the eigenvalue $\lambda_k^1$ of $\Phi_k$ converges to the unit circle. At $\alpha^*$, $F_{\alpha^*}(\cdot)$ is not exponentially stable anymore and have neutral trajectories.

$|\bar{\lambda}|$ is the maximal eigenvalue modulus of $H(\cdot)$ over $[0,T]$. In this case $|\bar{\lambda}| = 0.9$ and therefore the condition number of the matrix might reach $\exp\left(2|\bar{\lambda}|T\right) \approx 5 \cdot 10^{15}$. Indeed, the monodromy matrix condition number is approximately $10^{15}$. This ill conditioning does not only happen when $\alpha$ is close to $\alpha^*$ but over the entire interval $[0,\alpha^*]$. In such a situation, the Hamiltonian approach induces too many numerical instabilities.

### B. Flying wing

We study a thrust vectored flying wing model as described in [15] (with drag and lift coefficients from ). The flying wing state is composed of a velocity vector $v = (v_x, v_z)$, the pitch angle $\theta$, and the incidence angle $\alpha$ (see Figure 5). We design a path following controller $u = g(t,x)$ using the projection operator approach (as described in [16]) that stabilizes the flying wing around a periodic path $\mathbf{x}^*(\cdot)$ composed of a deceleration followed by an acceleration (both longitudinal). The path is described as a deceleration from $8m.s^{-1}$ to $1m.s^{-1}$ within $10s$ and acceleration from $1m.s^{-1}$ to $8m.s^{-1}$ within $10s$. The two motions are both separated by $10s$ and the periodic motion is repeated every $T = 40s$.

The closed-loop model of the flying wing can be described as the autonomous nonlinear system

$$\dot{\mathbf{x}} = f(t,\mathbf{x}). \tag{13}$$

We compute the state-to-state $H_\infty$ gain of the model linearized around $\mathbf{x}^*$. I.e. we compute the gain of $G_{i,j}$ defined in (1) with $A(t) = \left.\frac{df(t,x)}{dx}\right|_{x=x(t)}$ and with $B(\cdot) = B_j$ and $C(\cdot) = C_i$, where $B_j = e_j$, $C_i = e_i^\top$ for $i,j = 1,\ldots,4$ (where $e_l$, for $l = 1,\ldots,4$, are the canonical basis's vectors of $\mathbb{R}^4$). $H_\infty$ gains of systems $G_{i,j}$ for $i,j = 1,\ldots,4$ are given in Table I. The numerical integration of the PDRE and PDLE is implemented as a S-function in Matlab Simulink and integrated using a fourth order Runge Kutta numerical integration scheme. Algorithm 1 stops after 43 iterations in average when $tol = 1e-6$. The computation of each gain $G_{i,j}$, for $i,j = 1,\ldots,4$, takes 16 seconds in average on an Intel i5-8250U.

| $j$ \ $i$ | 1 | 2 | 3 | 4 |
|---|---|---|---|---|
| 1 | 0.491837 | 0.325122 | 0.195526 | 0.17978 |
| 2 | 1.45941 | 0.614567 | 0.215295 | 1.25802 |
| 3 | 1.33081 | 0.779088 | 0.778269 | 1.29261 |
| 4 | 0.111972 | 0.0623993 | 0.0671938 | 0.101557 |

TABLE I

State-to-state $H_\infty$ gains of flying wing system defined in Section V-B. $\|G_{i,j}\|_\infty$ corresponds to the $H_\infty$ norm between a disturbance over the $j^{th}$ state's dimension and observed through the $i^{th}$ state's dimension.

## VI. Conclusion

We described a method to estimate the $H_\infty$ gain of a Periodic Linear System. To do so, we compute an increasing sequence of solutions to a Periodic Differential Riccati Equation (PDRE) parametrized by the gain candidate. Solutions of the PDRE are then computed with a prediction-correction algorithm.

Working with the PDRE instead of using the Hamiltonian open new horizons such as the computation of $H_\infty$ norm for periodic systems subject to Integral Quadratic Constraint (IQC). For such systems, the knowledge of the PDRE's solution can be used to find necessary optimality conditions over the weights of the different IQCs.

The prediction step in the continuation method's algorithm can be improved by using Taylor expansions of a higher order. Higher derivatives of the PDRE according to the gain candidate can be computed. They are all solutions of a Periodic Lyapunov Differential Equation for which efficient numerical methods exist. Such an extension would allow us to take longer steps in the prediction-correction algorithm and therefore fewer iterations would be necessary to compute the $H_\infty$ gain.

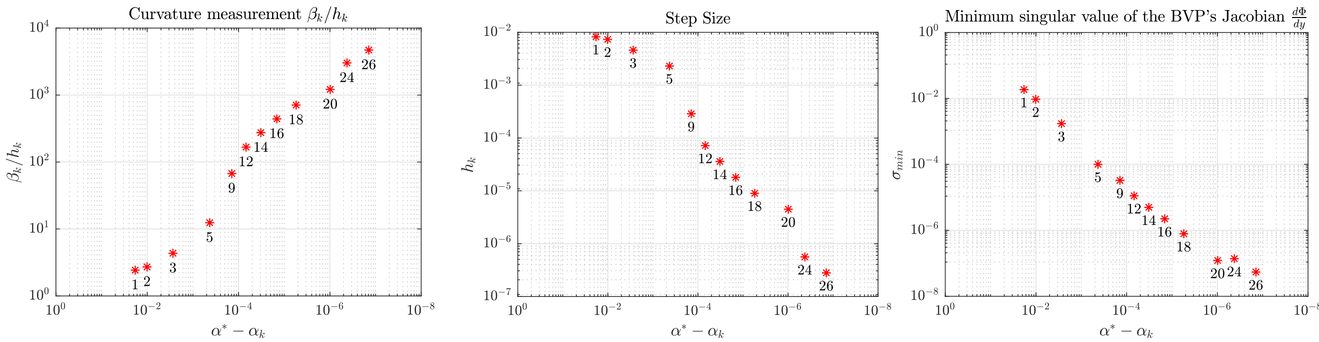


(a) Curvature (b) Step Size (c) Jacobian determinant of the BVP solver

Fig. 3. Plots (a), (b), and (c) depict internal states of Algorithm 1 with respect to iterations (at steps where the corrector successfully solved (5)). Each number below the markers correspond to the iteration value $k$. Each plot is in log-log scale with an abscissa corresponding to the distance of $\alpha_k$ to the optimal $\alpha^*$. The curvature (a) of $\alpha \to P_\alpha(\cdot)$ diverges as $\alpha \to \alpha^*$. (b) shows the step size $h_k$ of the continuation method. The tangent vector is not defined at $\alpha^*$. The Jacobian of the root-finding algorithm in the BVP solver (c) approaches noninversibility when $\alpha \to \alpha^*$.

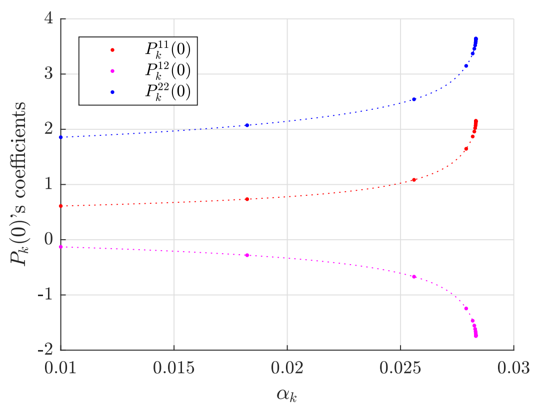


Fig. 4. Coefficients of $P_k(0)$ through iterations compared to their associated $\alpha_k$'s value. Dotted lines correspond to the continuous curves $\alpha \to P_\alpha^{ij}(0)$, $i, j \in \{1, 2\}$.

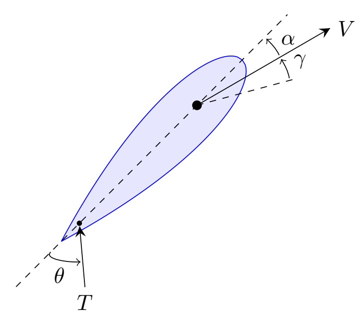


Fig. 5. Description of the vectored thrust flying wing model. $V$ is the velocity vector, $T$ is the thrust, $\theta$ is the direction of the thrust vector in the flying wing frame.

## APPENDIX

To use the projection operator method, we choose a smooth representation of the dynamical model of the flying wing, and its lift coefficient $c_L(\cdot)$ and drag coefficient $c_D(\cdot)$ are chosen as smooth functions of the angle of attack $a$, $C_{L1}(a) = \overline{c}_{L1} tanh\left(\frac{c_{L1}}{\overline{c}_{L1}}a\right)$, $C_{L2}(a) = \overline{c}_L sin\,(2a)$, $\varphi = \frac{1}{4}\,(1 + tanh\,(b(a + a_1))\,(1 - tanh\,(b(a - a_1))$, and $c_L(a) = \varphi(a)C_{L1}(a) + (1 - \varphi(a))C_{L2}(a)$, where $c_{L1} = 6.4$, $\overline{c}_{L1} = 1.3$, $a_1 = 33.5°$, and $b = 9$ and $c_D(a) = (\overline{c}_D - \underline{c}_D)\frac{1-cos(2a)}{2} + \underline{c}_D$ where $\overline{c}_D = 1.8$ and $\underline{c}_D = 0.02$. $c_L$ and $c_D$.

## REFERENCES


[1] C.C. Chung and J. Hauser, Nonlinear control of a swinging pendulum, *Automatica*, volume 31, 1995.
[2] C.C. Chung and J. Hauser, Nonlinear $H_\infty$ control around periodic orbits, *Systems & Control Letters*, volume 30, 1997.
[3] J. Nie, R. Conway, and R. Horowitz, Optimal $H_\infty$ control for linear periodically time-varying systems in hard disk drives, IEEE/ASME Transactions on Mechatronics, volume 18, 2013.
[4] P. Apkarian and D. Noll, Nonsmooth $H_\infty$ synthesis, *IEEE Transactions on Automatic Control*, volume 51, 2006.
[5] A. Varga, On solving periodic differential matrix equations with applications to periodic system norms computation, *Proceedings of the 44th IEEE Conference on Decision and Control*, 2005.
[6] J. Zhou and T. Hagiwara, $H_2$ and $H_\infty$ norm computations of linear continuous-time periodic systems via the skew analysis of frequency response operators, *Automatica*, volume 38, 2002.
[7] S. Richter, L.D. Davis, and E.G. Collins Jr, Efficient computation of the solutions to modified lyapunov equations, *SIAM Journal on Matrix Analysis and Applications*, volume 14, 1993.
[8] J.P. Schellhorn, An homotopy method for Riccati equations, *IFAC Proceedings*, volume 20, 1987.
[9] V.A. Tsachouridis, A complex line homotopy algorithm for coupled Algebraic Riccati Equations, *IMA Journal of Mathematical Control and Information*, volume 34, 2015.
[10] W.W. Lin, C.-S. Wang, and C.H. Han, Continuation methods for solving modified discrete-time Algebraic Riccati Equations, *IEEE Transactions on Automatic Control*, volume 40, 1995.
[11] E. Zeidler, Applied Functional Analysis, *Springer-Verlag*, volume 109, 1995.
[12] S. Bittanti, A.J. Laub, and J.C. Willems, The Riccati Equation *Springer-Verlag* , 1991.
[13] E.L. Allgower and Kurt Georg, Introduction to numerical continuation methods, *SIAM*, volume 45, 2003.
[14] J. Kierzenka and L.F. Shampine, A BVP solver that controls residual and error, *JNAIAM*, volume 3, 2008.
[15] J. Hauser and A. Jadbabaie, Aggressive maneuvering of a thrust vectored flying wing: A receding horizon approach, *Proceedings of the 39th IEEE Conference on Decision and Control*, volume 4, 2000.
[16] J. Hauser, A projection operator approach to the optimization of trajectory functionals, *IFAC Proceedings Volumes*, volume 35, 2002.